Turbulent Diffusion in the Core of Fully Developed Pipe Flow

LIONEL V. BALDWIN and THOMAS J. WALSH

Case Institute of Technology, Cleveland, Ohio

This paper summarizes an experimental study of turbulent diffusion downstream of a line source of heat. Mean temperature profiles in the core of nearly fully developed pipe flow were measured at four mean velocities, from U_o = 72.6 to 160 ft./sec. Hot-wire anemometer surveys showed that the turbulence in the axial core was nearly homogeneous and isotropic. The objective was to find empirical relations between the anemometer (Eulerian) specification of the turbulence and the Lagrangian statistical properties which determine diffusion.

The diffusion results agreed with predictions of G. I. Taylor's theory of diffusion by continuous movements; the eddy diffusivity increased from zero at the heat source to a constant, asymptotic value far downstream. The Lagrangian correlation coefficients inferred from the diffusion data had shapes similar to the Eulerian correlations over most of the range of time and space. Empirical relations were found to relate the coordinates of the Lagrangian and Eulerian correlation coefficients over the range of this experiment. In addition preliminary measurements are reported for a general Eulerian correlation which is a function of both space and time; the results indicate that a special case of this new Eulerian function may be a fair approximation of the Lagrangian correlation.

The axial core of air that is flowing steadily through a long circular pipe is a region of nearly homogeneous, isotropic turbulence. Homogeneous, isotropic turbulence is a very special type of turbulent flow which has received a great deal of attention in the literature during the last decade. The stimulus for this research was the theoretical work of G. I. Taylor (*1*) in 1935. However nearly all of the literature describing the development of the theory of homogeneous, isotropic turbulence (*2, 3, 4, 5, 6*) has dealt with the dynamics of turbulent kinetic-energy losses in grid produced turbulence in wind tunnels. On the other hand chemical engineers are usually interested in another aspect of turbulent phenomena, the dispersion of mass or heat by turbulent diffusion. The study of turbulent diffusion that is presented here was designed to obtain diffusion data in the simplest form of turbulent flow, nearly homogeneous isotropic turbulence that is stationary in time. Owing to the simplicity of the chosen experimental model, it is possible to use the theory of diffusion by continuous movements (*7*) as a theoretical model and to test the theoretical concepts experimentally.

The objective of this work is easily stated: to determine turbulent diffusion parameters from a statistical description of the turbulence as measured by fixed probes. Since the turbulence considered approaches the simplest form (homogeneous and isotropic), it is surprising at first glance that theoretical attacks on this problem have all failed. The basic difficulty is twofold. In the first place the statistical description of a turbulent field requires a knowledge of the complete joint probability distribution function for the velocity components (x, y, z directions) at all points in space (3, p. 12; 2, p. 18). The statistical functions usually measured and reported are the correlation functions which refer to two points in space. The correlation (or spectrum) functions dominate current theory and experiment because of their simplicity and do not describe the turbulence completely even in a statistical manner (*3*). Secondly to pass from the Eulerian description of the flow (fixed probes) to the Lagrangian description of the motion of an element of volume (turbulent diffusion) requires a solution of the Navier-Stokes equations. Thus the total difficulty is not only the nonlinearity of the partial differential equations of motion but also the incomplete initial conditions.

To circumvent the missing theoretical link two distinct viewpoints of the turbulent motion are used. The Eulerian description has received the most attention (for example *2, 3*). In this research the authors seek empirical relations between this Eulerian description and the Lagrangian statistical functions which are used in the diffusion analysis. The following paragraph is a brief summary of the results of the Lagrangian analysis of diffusion by continuous movements (*7*).

Imagine that a fluid element is tagged at the origin of the x-, y-, z-coordinates at some time $t = 0$ in a box of stationary turbulence. Then this fluid element at some dispersion time t later has moved to a point $P(X, Y, Z)$, whose coordinates are equal to

$$X = \int_0^t u_{La}(t')dt',\ Y = \int_0^t v_{La}(t')dt',$$
$$Z = \int_0^t w_{La}(t')dt' \qquad (1)$$

Since the fluid is at rest except for the turbulence, the time mean displacements over all the particles have the same properties as the mean turbulent velocity; that is $\overline{X} = \overline{Y} = \overline{Z} = 0$. However the displacement variances will depend on the dispersion time. For example in the y-direction

$$\frac{1}{2}\frac{\overline{dY^2}}{dt} = \overline{\frac{dY}{dt}Y} = \overline{v_{La}(t)\int_0^t v_{La}(\tau)d\tau} \qquad (2)$$

Here the superscript bar indicates an average (over many particles) of individual particle histories. But $v_{La}(t)$ is not a function of τ, so

$$\frac{1}{2}\frac{\overline{dY^2}}{dt} = \int_0^t \overline{v_{La}(t)v_{La}(\tau)}d\tau \qquad (3)$$

When the average motion of a great many fluid particles (tagged at $t = 0$ at the origin) is considered, the mean velocity product may be written in terms of the Lagrangian correlation coefficient:

$$\frac{1}{2}\frac{\overline{dY^2}}{dt} = \overline{v^2_{La}}\int_0^t \mathcal{R}(\tau)d\tau \qquad (4)$$

Finally the desired equation for the variance $\overline{Y^2}$ is

$$\frac{1}{2}\overline{Y^2} = \overline{v^2_{La}}\int_0^t \left[\int_0^{t''} \mathcal{R}(\tau)d\tau\right]dt' \qquad (5)$$

where the prime and τ notation merely distinguishes between the variable and the limit in each integration. Owing to the isotropy of the motion

$$\overline{Y^2} = \overline{X^2} = \overline{Z^2}$$

Of course the specification of the mean concentration distribution in space and time which is produced by the turbulent motion is the objective of an ordinary diffusion analysis. The dispersion of the particles tagged at the origin at

Lionel V. Baldwin is at Lewis Research Center, National Aeronautics and Space Administration, Cleveland, Ohio.

$t = 0$ is assumed to be a three-dimensional Gaussian function:

$$c(x, y, z, t) = \frac{1}{(2\pi\overline{Y^2})^{3/2}}$$

$$\exp\left[-(x^2 + y^2 + z^2)/2\overline{Y^2}\right] \quad (6)$$

The concentration c is defined here as the fraction of the total number of particles tagged, which at some time t later are at the point x, y, z. The mean concentration at a point depends on the variance $\overline{Y^2}$ and its functional relation with the dispersion time t. Equation (5) shows that $\overline{Y^2}$ is given in terms of the Lagrangian correlation coefficient $\mathcal{R}(\tau)$ and the Lagrangian velocity variance $\overline{v^2}_{La}$. Thus the prediction of the mean concentration in turbulent diffusion depends on the characterization of the turbulent motion by these two Lagrangian statistical properties. Conversely the Lagrangian statistical properties must be inferred from concentration measurements.

The extension of the Taylor theory to a variety of initial conditions has been published by Frenkiel (*8*) and Mickelsen (*9*).

References to previous experimental work closely related to this research may be summarized as follows: channel flow (10), pipe flow (*11, 12, 13*), wind tunnel grid turbulence (*14, 15, 16*), and atmospheric diffusion (*17, 18, 19, 20*).

EXPERIMENTAL APPARATUS AND PROCEDURE*

Ducting and mean airflow measurements

A 35-ft. section of 8-in. diameter commercial pipe was used at the inlet of the test section to approach a nearly fully developed pipe flow. Room air was drawn through inlet filters to remove suspended dust. The incoming air passed over a 2-ft. pipe section coated with coarse sandpaper to promote the growth of the turbulent boundary layer. Following the long inlet section the air flowed through a 4 ft. long test section of similar 8-in. pipe which was drilled and tapped for instrumentation access. The exit flow at essentially ambient pressure passed through a choked exhaust plate; downstream of the plate the pressure was maintained at 10 in. of mercury absolute by the laboratory exhaust facility. Therefore small fluctuations in exhaust pressure did not affect the flow rate; the inlet filters damped room drafts. The mean flow rate was controlled by varying the exhaust plate open area.

The two dimensionality of the central diffusion wake simplifies the choice of coordinate systems. A rectangular Cartesian system is used herein with the origin at the intersection of the pipe's axial center line and the vertical line source of heat, which was located in the test section inlet. The x-direction is measured from the origin in the mean flow direction; the y-direction is the lateral distance from the axial center line in the horizontal plane.

The mean flow velocity was surveyed with a total static pitot probe. In the experimental procedure the mean velocity at the pipe center line was the primary flow variable. The air was at ambient temperature and pressure. Four velocities were used: 72.6, 106, 135, and 160 ft./sec. This procedure gave a range of turbulent velocities $\overline{v^2}$ and a slight variation in the Eulerian scales of the turbulence. Turbulence and diffusion measurements were performed at all four flow conditions.

Hot-wire anemometer instruments and techniques

The hot-wire anemometer amplifier, which was used, was of the constant-temperature type. The auxiliary equipment includes a true root-mean-square voltmeter, dual channel tape recorder, and autocorrelation computer (*22, 23, 24*).

The hot-wire used was a 0.080-in. long sample of 0.00020-diam. tungsten wire. The heat transfer characteristics of the hot wire govern its sensitivity to the flow variables, and this has been the subject of a series of papers in the last two years (*25, 26, 27, 28*). The method described in the referenced reports and used here differs from the traditional treatment (that is King's equation, reference 29) and is expected to yield a more accurate value of turbulence intensity. Fortunately all nondimensional groupings of anemometer data, such as correlation coefficients, are not affected by uncertainty of previous wire calibration procedures because linearized anemometry techniques are usually employed.

The procedure included a detailed survey of the turbulent pipe core with the hot-wire anemometer.

Heat source and diffusion measurements

The ideal line source of heat would have negligibly small diameter and would not disturb the turbulent field. However in order to transfer a detectable amount of heat into the stream the heat source must be a hot wire of appreciable dimensions. Three diameter sources were used at each flow rate; these were 0.010, 0.020, and 0.040 in. (also 0.065 at $U_e = 160$). This procedure gives sufficient data so that the ideal source can be approximated by extrapolating the diffusion data to zero source diameter. The resistance heat sources were 7½-in. long samples of constantan wire with copper electrical connectors at each end. The wires were held taut by weights.

The temperature profile of the diffusion wake was measured across the pipe diameter in the y-direction by thermopile traverses at Δx-intervals of 2 in. Six iron-constantan thermocouples were alined vertically where the wake temperature was constant. This thermopile output was bucked against a reference thermopile at the ambient temperature. The bucking voltage was proportional to the temperature rise in the wake, and it actuated the pen travel on the 0 to 1-mv. range of an automatic X-Y recorder. The probe actuator travel across the wake was proportional to the chart travel. This combination of six element thermopiles and standard automatic potentiometer formed a surprisingly sensitive and reproducible measuring technique for the diffusion wake which had a maximum temperature rise of less than 10°F. and which was about 2½-in. wide at its maximum spread.

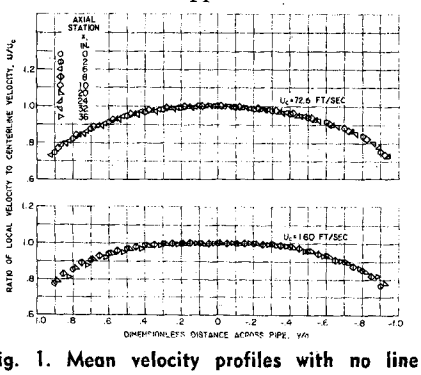

Fig. 1. Mean velocity profiles with no line source.

RESULTS AND DISCUSSION

Test for Fully Developed Pipe Flow

The most direct test for the existence of fully developed flow is an unchanging velocity profile for increasing axial distances. If the mean velocity profiles at a given flow rate do not change over the 4-ft. length of the test section, then it follows that nearly fully developed flow was attained in this experiment. Figure 1 shows that this criterion was well satisfied at the two extreme flow rates.

A slight asymmetry is evident in all the profiles, which show higher velocities for $0 < y/a < +0.3$ than those recorded on the -0.3 side. The deviation from symmetry is small, but it occurs consistently at all flow rates and therefore must be regarded as real.

Turbulence in the Axial Core

Isotropy. The most direct test for isotropy is to contrast the lateral intensity with the longitudinal intensity. The lateral $\sqrt{\overline{v^2}}/U_c$ and longitudinal $\sqrt{\overline{u^2}}/U_c$ intensities were calculated from three root-mean-square readings from a single anemometer wire operated at three yaw angles to the flow (135, 90, 45 deg) as described in reference *21*. The data scatter was much worse than in the remainder of the anemometer data, but the $\sqrt{\overline{v^2}}/\sqrt{\overline{u^2}}$ results were consistently below 1; $\sqrt{\overline{v^2}}/\sqrt{\overline{u^2}} \approx 0.8$ to 0.7 along the center line. This compares favorably with a summary of the results of previous workers (23) who found $\sqrt{\overline{v^2}}/\sqrt{\overline{u^2}}$ varied between 0.9 and 0.7 along pipe center lines.

The pipe core turbulence departs from isotropy by about 30% if $\sqrt{\overline{v^2}}/\sqrt{\overline{u^2}}$ is used as a criterion.

* See (*21*).

The departure of the pipe core from isotropy should be compared with results of grid turbulence, when one considers the relative merits of experimental simulations of isotropic flow. Grant and Nisbet (*30*) observed that $\sqrt{\overline{v^2}}/\sqrt{\overline{u^2}}$ was about 0.85 downstream of a 2-in. square mesh grid at two flow velocities.

In the diffusion experiment the lateral dispersion is measured, but the axial dispersion is essentially neglected. Therefore a slight anisotropy is not serious; the primary requirement is homogeneity of $\sqrt{\overline{v^2}}$.

Homogeneity. Anemometer surveys showed that the longitudinal intensity along the center line is independent of the axial station for all flow velocities. Figure 2 shows that the longitudinal intensity rises only 15% at the lateral extremes of the 2-in. core of interest in the diffusion experiment. The variation of $\sqrt{\overline{u^2}}$ and $\sqrt{\overline{v^2}}$ reported by Sandborn (Figures 10 and 13 of reference 23) shows that $\sqrt{\overline{v^2}}$ does not change as rapidly as $\sqrt{\overline{u^2}}$ near the center line. Furthermore measurements of $\sqrt{\overline{v^2}}$ along the center line were made at 2, 17, and 32 in. in the present experiment. Although the data scatter was about ± 10%, no systematic variation of $\sqrt{\overline{v^2}}$ along the center line was discernible. It is concluded that the 2-in. diameter core of the pipe is a region of homogeneous, stationary turbulence along the axial center line, and departures from homogeneity from 5 to 15% are indicated by the intensity profiles across the central core in the y-direction.

Intensity. The longitudinal intensity $\sqrt{\overline{u^2}}/U_c$ at the center line was 3.5% for all mean flow rates. This value is higher than previously reported values (23), which were 2.5% over the same pipe Reynolds number range. The discrepancy is primarily due to differences in anemometer calibration procedures, which were discussed previously. $\sqrt{\overline{u^2}}/U_c = 0.035$ is regarded as correct.

Eulerian correlation coefficient. Perhaps the most important additional statistical property obtained from the analysis of the anemometer signal is the Eulerian autocorrelation coefficient. A representative sample of these data is presented in Figure 3. These autocorrelation curves are plotted automatically by an X-Y recorder in an analogue computer. The autocorrelation coefficient is a function of the delay time introduced at the analogue computer between otherwise identical

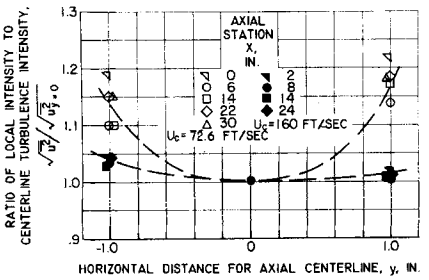

Fig. 2. Longitudinal turbulence intensity profiles across pipe core.

signals from a single anemometer which is sensitive to the longitudinal turbulent velocity. However Taylor (*1*) introduced an approximation, early in the development of the statistical theory, which relates the autocorrelation to a space Eulerian correlation coefficient $f(\xi)$. Taylor's hypothesis (*31*) states that the structure of a turbulent eddy changes little during the time necessary for the eddy to pass over a single wire. Therefore the autocorrelation coefficient at a time delay Δt_1 should approximate $f(\xi_1)$, where $\xi_1 = U\Delta t_1$ and U is the mean flow velocity. The hypothesis has been tested experimentally (for example reference 32) with good results. The data shown in Figure 3 were all obtained by transforming the time axis of the autocorrelations into the space axis of the Eulerian correlation with $\xi = Ut$.

Effect of line source on turbulent intensity. All the turbulence measurements reported to this point were made in the absence of the wire heat source used in the diffusion experiment. The vortices generated by the heat source lower the local mean velocity and increase the turbulence, so the center line intensity is roughly doubled at extreme conditions. This turbulent disturbance decays completely about 6 in. downstream. As mentioned earlier the diffusion results were extrapolated to zero source diameter to minimize this effect.

Lagrangian Statistical Properties from Diffusion Results

Four typical examples of the mean temperature traces downstream of the heat source are shown in Figure 4. These traces are copies of recorded data as obtained on the X-Y reactor. Note the good agreement between the traces for probe travel in both directions across the wake, as shown by the two lines of each profile.

The data reduction from the profiles to the desired turbulence displacement variance $\overline{Y^2}$ is a straight-forward but time consuming process. The mean temperature rise (above ambient) ΔT is read for various distances Δy measured from the pipe center line. These individual points from the profile are then replotted on semilog graph paper with $\Delta T/\Delta T_0$, which is the ratio of the temperature rise to the peak temperature difference ΔT_0, as ordinate, and the abscissa is the square of the probe displacement from the pipe center line $(\Delta y)^2$. The slopes of the straight lines in the semilog plot are directly related to the total displacement variance $\overline{Y^2}_{tot}$. Both Mickelsen (*12*, p. 6) and Uberoi and Corrsin (*15*, p. 9) have shown that the variance of a profile downstream a distance x from a continuously heated source is closely equivalent to the variance of the cloud of tagged particles released at the source at a time interval t earlier; that is since $\sqrt{\overline{v^2}}/U << 1$ for the flow studied, axial diffusion can be neglected and the variance of the measured profile at x is equal to $\overline{Y^2}_{tot}$ of Equation (5) at $t = x/U$. Therefore the following equations may be written:

$$\frac{\Delta T}{\Delta T_0} = e^{-(\Delta y)^2/2\overline{Y^2}_{tot}} \qquad (7)$$

where

$$\overline{Y^2}_{tot} = \overline{Y^2} + 2\left(\frac{x}{U}\right)\alpha \qquad (8)$$

and

$$\frac{1}{2}\overline{Y^2} = \overline{v^2}_{La}\int_0^{x/U}\left[\int^{x''/U} \mathcal{R}\left(\frac{x''}{U}\right)d\left(\frac{x''}{U}\right)\right]d\left(\frac{x'}{U}\right) \qquad (9)$$

It follows from Equation (7) that the slopes of the semilog working plots are equal to $(-1/2\overline{Y^2}_{tot})$. Then with Equation (8) and the thermal diffusivity α from (*33*), $\overline{Y^2}$ was calculated; the maximum correction for molecular diffusion was 3%. An interaction of turbulent and molecular motion, accelerated diffusion, has been proposed by Townsend (*16*, *34*). However recent experiments seem to justify Equation (8) for all x/U except perhaps very near the source (*35*).

The summary of the results obtained in this manner at one of the four mean flow conditions is given in Figure 5, where each data point is the result of reading an entire profile. At each mean velocity similar results were obtained. Three different heat sources were used, and the data are distinguished by different symbols for each source diameter. The smooth curve drawn on Figure 5 is not intended to be the best curve through the data. Rather the initial portion of each curve was obtained by extrapolating cross plots of the data to zero source diameter. For distances far downstream of the source this zero source extrapolation was not practical because the profiles from the smallest

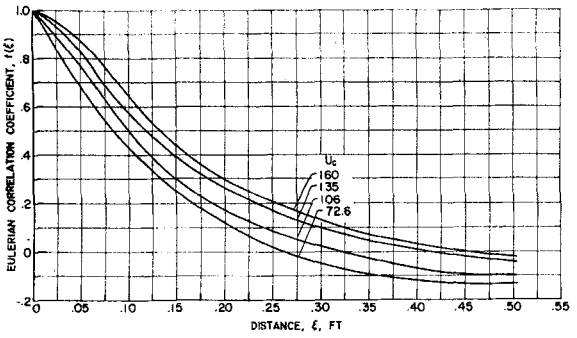

Fig. 3. Typical Eulerian correlation coefficients of the longitudinal turbulent velocity at each mean flow velocity. ξ measured along pipe center line.

source had too low a peak temperature. Data scatter also became severe at large distances from the source, which is mostly attributable to profile readability. Therefore the curve shown for times far from the source represents a judgment for the best continuation of the initial curve (for a perfect source) relative to the data from imperfect sources.

Equation (9) shows that one-half times the measured displacement variance $\frac{1}{2}\overline{Y^2}$ is equal to the product of the Lagrangian velocity variance $\overline{v^2_{La}}$ and the double integral of the Lagrangian correlation coefficient $\mathcal{R}(\tau)$. Therefore to infer the Lagrangian correlation from the measured data requires the equivalent of a double differentiation. Several schemes have been used by previous investigators to obtain consistent results despite the severity of two differentiations of experimental data. An integration technique was adopted here which is similar in some respects to the method used by Mickelsen (*12*). Essentially the method finds a Lagrangian correlation coefficient whose double integral [Equation (5)] checks the measured $\frac{1}{2}\overline{Y^2}$. The measured Eulerian correlation curves serve as a convenient starting point for what is basically a trial-and-error search for this Lagrangian correlation coefficient. Consider the following equation as the definition of a factor K which is to be found:

$$\int_0^{K\xi}\left[\int_0^{K\xi'} f(K\xi'')\,d(K\xi'')\right]d(K\xi') = \frac{1}{2}\overline{Y^2} = \overline{v^2_{La}}\int_0^t\left[\int_0^{t''}\mathcal{R}(\tau)\,d\tau\right]dt' \qquad (10)$$

In general K will not be a constant in the left-hand integrations. However if the integration is performed numerically by dividing the $f(\xi)$ curve and the $\frac{1}{2}\overline{Y^2}$ curve into an equal number of small increments, then K may be considered as a constant for each increment. In this manner the numerical integration makes it possible to estimate K as a function of ξ with good precision by simply increasing the number of increments in the numerical integration.

The total time interval is defined from $t=0$ to $t=\tau_n$, where $d\left(\frac{1}{2}\overline{Y^2}\right)/d\tau$ is initially constant. This interval is divided into a convenient number of equal time increments (20 to 30 depending on the $\frac{1}{2}\overline{Y^2}$-curve). The corresponding $f(\xi)$ curve for that flow condition is divided into an equal number of distance increments between $\xi = 0$ and $\xi = \xi_n$, where the $f(\xi)$ function first intersects zero, $f(\xi_n) = 0$. Then the numerical integration proceeds when one assumes that K is constant only over each increment but that the empirical factor is allowed to vary from increment to increment. A summary of the K factors found in this manner is given in Figure 6, where a continuous curve has been drawn through the incremental K values found in the step by step integration. It is possible to plot the new function $f(K\xi)$ from these results which satisfies Equation 10, and this new function is equal to $\mathcal{R}(\sqrt{\overline{v^2_{La}}}\,\tau)$ because $\sqrt{\overline{v^2_{La}}}$ is not a function of τ. But $\sqrt{\overline{v^2_{La}}}$ is readily available because the prescribed limits of the double integration occur at $f(K_n\xi_n) = \mathcal{R}(\tau_n) = 0$. Therefore

$$\sqrt{\overline{v^2_{La}}} = \frac{K_n\xi_n}{\tau_n} \qquad (11)$$

and in general

$$f\left(\frac{K\xi}{\sqrt{\overline{v^2_{La}}}}\right) = \mathcal{R}(\tau) \qquad (12)$$

Figure 7 shows the Lagrangian correlation coefficients $\mathcal{R}(\tau)$ which were found in the manner described above

Table 1 lists the corresponding Lagrangian root-mean-square velocities. These results were checked against the experimental $\frac{1}{2}\overline{Y^2}$ functions with Equation 9; the agreement between the calculated $\frac{1}{2}\overline{Y^2}$ curves and the experimental curves was within 5% over the entire range for each mean velocity. It is possible to conclude therefore that the Lagrangian correlation coefficients and velocity variances have been found which are consistent with the smoothed diffusion data.

Comparison of Lagrangian and Eulerian Correlation Coefficients

Not only are the K-curves shown in Figure 6 part of a convenient method for finding the Lagrangian correlation coefficient but they also give an interesting empirical relation between the Lagrangian and Eulerian correlation coefficients. The hypothesis which prompted the adoption of the K-technique was that the Eulerian and Lagrangian correlation coefficients might have similar shapes. The nearly constant values found for the K factor over the major portion of ξ show that the hypothesis was reasonable. However the twofold variation of the empirical factor K with mean flow velocity over the small range of this experiment certainly limits its utility. The similarity in shape of $f(\xi)$ and $\mathcal{R}(\tau)$ is qualitative and fails completely at large separation distances where $f(\xi)$ becomes negative. This failure suggests that nothing fundamental should be implied from the empirical comparison. Nevertheless there is a definite need for engineering approximations of eddy diffusivities from hot-wire measurements of the turbulence, and Figure 6 represents an attempt to fill this need. Mickelsen (*12*) was the first to seek relations of this type; he measured helium concen-

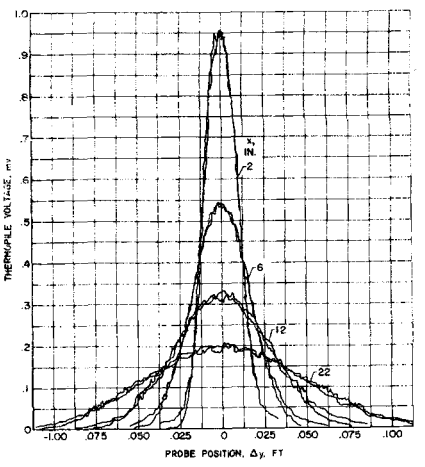

Fig. 4. Typical traces of mean temperature profiles; U_c = 160 ft./sec. and 0.040-in. diameter heat source.

Table 1. Summary of Scales, Intensities, and Eddy Diffusivities Statistical Properties

	Eulerian		Lagrangian		Comparison		Eddy diffusivity
U_c	$\sqrt{\overline{u^2}}/U_c$ none	L_f, ft.	$\sqrt{\overline{u^2_{La}}}/U_c$ none	$\mathcal{L}$, ft.	$L_f/\mathcal{L}$ none	$\sqrt{\overline{v^2_{La}}}/\sqrt{\overline{u^2}}$ none	D, sq. ft./sec.
72.6	0.035	0.0978	0.027	0.0277	3.5	0.77	0.054
106	0.035	0.116	0.029	0.0232	5.0	0.83	0.072
135	0.035	0.142	0.028	0.0236	6.0	0.80	0.088
160	0.035	0.154	0.032	0.0236	6.5	0.91	0.12

tration profiles downstream of a point source in the core of an 8-in. pipe. British workers in atmospheric diffusion have given similar empirical relations (*18*). A new analysis of Mickelsen's results is presented in reference *21*; his diffusion data yielded *K*-factors which ranged from about 0.5 at $U = 50$ to 0.2 at $U = 160$ ft./sec.; that is Mickelsen's helium diffusion data agree qualitatively with the present results. The quantitative discrepancy may be caused in part by differences in the degree of development of the pipe flow and in diffusion source disturbances of the turbulence.

Comparison of Lagrangian and Eulerian Scales and Intensities

The relative magnitudes of the integral scales are readily determined. The Eulerian integral scale is defined here as the area under the $f(\xi)$ curve for all $f(\xi) > 0$. The portion of negative correlation is eliminated in this definition. If ξ_n is the value of ξ where $f(\xi)$ first equals zero, then

$$L_f = \int_0^{\xi_n} f(\xi)\,d\xi \qquad (13)$$

The $f(\xi)$ curves were given earlier as Figure 3. The analogous Lagrangian length scale is defined as

$$\mathcal{L} = \sqrt{\overline{v^2_{La}}} \int_0^{\tau_n} \mathcal{R}(\tau)\,d\tau \qquad (14)$$

where $\tau = \tau_n$ at $\mathcal{R}(\tau) \approx 0$. As mentioned earlier the Lagrangian correlation coefficients are given in Figure 7, and the root-mean-square velocities are listed in Table 1.

Table 1 also lists the results of the comparison of integral scales. The Eulerian scale increases with mean flow velocity, while the Lagrangian length characteristic is apparently constant for all flow rates studied. The net result is that the ratio of Eulerian to Lagrangian integral scales increases from 3.5 to 6.5 as U_c varies from 72.6 to 160 ft./sec.

The comparison of Lagrangian to Eulerian intensities is given in Table 1 as the ratio $\sqrt{\overline{v^2_{La}}}/\sqrt{\overline{u^2}}$. The Lagrangian lateral intensities inferred from the diffusion results vary nonsystematically from about 80 to 90% of the anemometer longitudinal intensity over the experimental range. No physical significance is attributed to these deviations because the accuracy of the individual intensities is probably no better than ±5%. However the ratio of $\sqrt{\overline{v^2_{La}}}/\sqrt{\overline{u^2}}$ is consistently smaller than unity, which agrees with the ratio of the anemometer lateral to longitudinal intensities.

Eddy Diffusivity

The relation between the concept of an eddy diffusivity, which is frequently used in engineering, and the theory of diffusion by continuous movements is worth noting. In Taylor's theory the assumption of Gaussian concentration distribution is usually justified by an analogy with molecular diffusion. The mean square displacement $\overline{Y^2}_{mol}$ for a particle in Brownian motion is given by the Einstein equation:

$$\overline{Y^2}_{mol} = (2D_{mol})t \qquad (15)$$

In the derivation of Einstein it is assumed that the jump time under consideration is much greater than an interval over which appreciable correlation exists between the velocity of the particle at the beginning and end (*36*). In this sense the Einstein equation is a limiting law. The molecular diffusion coefficient can be expressed in terms of the mean molecular velocity and the mean free path, so for air (*37*)

$$D_{mol} = 0.57\,\bar{c}\,\bar{l} \qquad (16)$$

An analogous set of relations can be derived for a limiting case of turbulent diffusion by continuous movements. Integration of Equation (5) by parts, with

$$\Phi \equiv \int_0^{t'} \mathcal{R}(\tau)\,d\tau \text{ and } d\theta \equiv dt' \qquad (17)$$

gives an alternate form

$$\frac{1}{2}\overline{Y^2} = \overline{v^2_{La}}\,t \int_0^t \mathcal{R}(\tau)\,d\tau - \overline{v^2_{La}} \int_0^t \tau\mathcal{R}(\tau)\,d\tau \qquad (18)$$

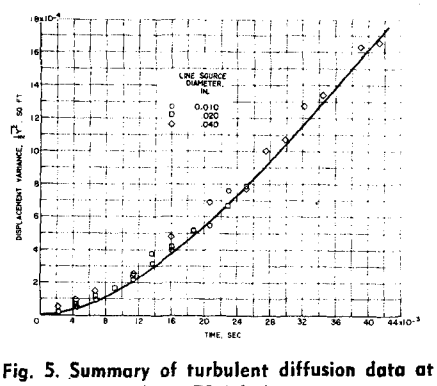

Fig. 5. Summary of turbulent diffusion data at $U_c = 72.6$ ft./sec.

The special case to be considered is for dispersion times larger than τ_n, where $\mathcal{R}(\tau)$ is essentially zero. In Equation (18) for $\tau > \tau_n$ the left integral is the Lagrangian scale [Equation (14)], and the right integral is simply the first moment of this scale; both integrals are numerical constants. For $\tau >> \tau_n$ the constant from the first moment of the scale becomes negligibly small compared with the linear term, so

$$\overline{Y^2} \approx (2\sqrt{\overline{v^2_{La}}}\,\mathcal{L})t \quad (t >> \tau_n) \qquad (19)$$

or

$$\overline{Y^2} \approx (2D)t \text{ where } D = \sqrt{\overline{v^2}}\,\mathcal{L} \quad (t >> \tau_n) \qquad (20)$$

Thus the eddy diffusivity is a constant for large dispersion times in accordance with Taylor's theory, and the analogy between $L \leftrightarrow l$ and $\sqrt{\overline{v^2_{La}}} \leftrightarrow \bar{c}$ is striking. Batchelor and Townsend (*34*, p. 359) give a detailed presentation of the limitations of this analogy. If an eddy diffusivity is defined for $t \leq \tau_n$, then D is no longer constant but varies with dispersion time thereby losing some of its utility (*9*).

The constant slope of the $\overline{Y^2}$ data at large times is evident in Figure 5; similar results were obtained at all four mean velocities. Thus the prediction of Equation (19) is verified experimentally. In general $D \approx 7.1 \times 10^{-4} U_c$ sq.ft./sec. for this experimental range of pipe Reynolds numbers, that is 2.8×10^5 to 6.4×10^5. The proportionality of eddy diffusivity to mean flow velocity in pipe flow has been proposed by Taylor (*38*) and also Hanratty et al. (*13*). By dimensional analysis they reasoned that the group $D/U_c 2a$ should be some function of pipe Reynolds number. A summary of previous experimental results verifies this functional dependence. At high Reynolds numbers, say above 5×10^4, $D/U_c 2a$ approaches a constant value of 8.2×10^{-4} and is independent of N_{Re} (*13*). The eddy diffusivities of Table 1 agree qualitatively with Hanratty's summary (*13*), but $D/U_c 2a$ is 1.1×10^{-3} or about 20% higher.

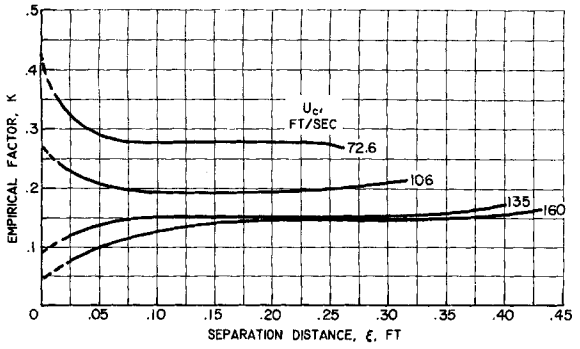

Fig. 6. Empirical factor relating Eulerian and Lagrangian correlation coefficients.

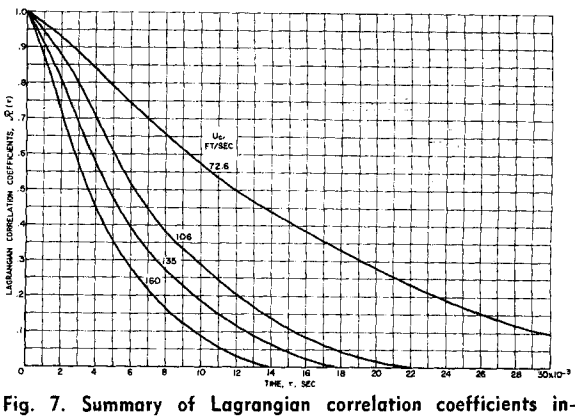

Fig. 7. Summary of Lagrangian correlation coefficients inferred from turbulent diffusion data.

Possible Improvements for Future Lagrangian and Eulerian Empirical Relations

It would be very desirable to have an Eulerian correlation coefficient which approached the true Lagrangian correlation. If such an Eulerian measure could be found, empirical generalizations relating hot-wire measurements to diffusion parameters would follow more readily. Burgers (*39*) has suggested an Eulerian correlation coefficient which may approach the true Lagrangian coefficient.

The flow in the axial core of the pipe flow is nearly homogeneous and isotropic, and it is stationary in time. Burgers considers the motion of fluid particles in such a flow having a mean velocity U; Figure 8 is an aid to the discussion. First consider the two types of Eulerian correlation coefficients for the lateral velocity v which have been reported in the past. The Eulerian correlation between fluid particles observed at the same instant of time at various values of x can be measured by two probes. In Figure 8 wire 1 at P measures particle (b) at the same instant wire 2 at Q sees particle (d). The instantaneous two-wire Eulerian correlation function for the transverse velocities where $\overline{PQ} = \xi$ then is

$$R_v(\xi) = \frac{\overline{v_b(x,t)v_d(x+\xi,t)}}{\overline{v^2}} \qquad (21)$$

The average is performed over many pairs of particles (that is long time averages); the subscript indicates the fluid particles of Figure 8 for emphasis. In Karman-Howarth (*5*) notation $R_v(\xi) = g(\xi)$.

Alternately with a single probe it is possible to consider all the particles passing over this fixed point. The single-wire Eulerian autocorrelation function for wire 1 at P in Figure 8 is

$$R_v(\tau) = \frac{\overline{v_b(x,t)v_a(x,t+\tau)}}{\overline{v^2}} \qquad (22)$$

The averaging is again over many pairs of particles.

The new Eulerian correlation function which Burgers proposed is a more general one. The instantaneous product of turbulent velocities for this general Eulerian correlation refers to two particles separated in time and space. For example in Figure 8 one point of this two dimensional Eulerian function would be defined by

$$R_v(\xi,\tau) = \frac{\overline{v_b(x,t)v_c(x+\xi,t+\tau)}}{\overline{v^2}} \qquad (23)$$

The averaging would be performed over many pairs of particles like (b) and (c) of this example.

Before discussing the properties expected for this general Eulerian correlation function one should recall the definition of the true Lagrangian single-particle correlation coefficient $\mathcal{R}(\tau)$. It may be written

$$\mathcal{R}(\tau) = \frac{\overline{v_b(t)\, v_b\,(t+\tau)}}{\overline{v^2_{La}}} \qquad (24)$$

The averaging is performed over many single particle time histories, of which particle (b) is an example from Figure 8.

Burgers suggested that in the case considered the Lagrangian time derivative of the transverse velocity is approximately given by

$$\frac{dv}{dt} \cong \frac{\partial v}{\partial t} + U\frac{\partial v}{\partial x} \qquad (25)$$

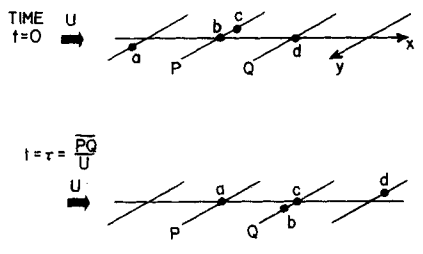

Fig. 8. Sketches for discussion fo Eulerian space-time correlations.

To the same approximation the Lagrangian correlation function $\mathcal{R}(\tau)$ will approach the Eulerian correlation function $R_v(\xi,\tau)$, where $\xi = U\tau$ in the latter. An appendix gives the detailed development of this approximate relation between $\mathcal{R}(\tau)$ and $R_v(\xi,\tau)\Big|_{\xi=U\tau}$.

Naturally the question is how good an approximation is Equation (25) and the resulting relation between correlation functions. Three terms in the complete Lagrangian derivative are neglected:

$$u\frac{\partial v}{\partial x} + v\frac{\partial v}{\partial y} + w\frac{\partial v}{\partial z}$$

These second-order terms may not be small compared with the difference between the large terms $\left|\frac{\partial v}{\partial t}\right|$ and $U\left|\frac{\partial v}{\partial x}\right|$ (*31*). The only true test of the approximation, or indeed any other assumption concerning mathematical models of physical problems, is whether experiment verifies the relation as useful.

A preliminary comparison of the general Eulerian correlation with the true Lagrangian correlation was the subject of the concluding experiment of this work. Two hot-wire anemometers separated in the axial direction by multiples of 2 in. were placed on the center line of the pipe in a mean flow of 75 ft./sec. The signals from the two wires were analyzed on an autocorrelation computer, and the results are given in Figure 9.

The peak correlation for the time delayed signals in Figure 9 occurs at a time delay τ which is approximately equal to ξ/U. The peaks all fall within 10% of this prediction but appear to be occurring at systematically larger time delays than predicted. Secondly the section of the general Eulerian correlation, which is defined by the peaks along $\xi = U\tau$, has a very gradual slope compared with either the single-wire Eulerian autocorrelation ($\xi = 0$) or the

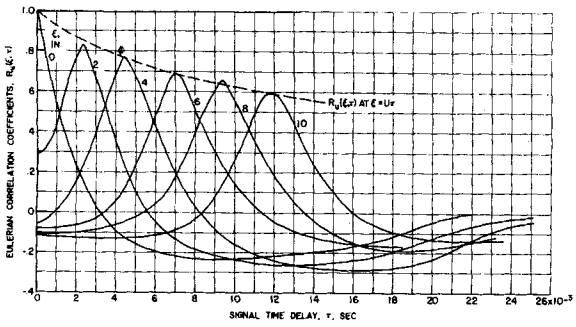

Fig. 9. General Eulerian correlation coefficient as a function of space and time; $U_c = 75$ ft./sec.

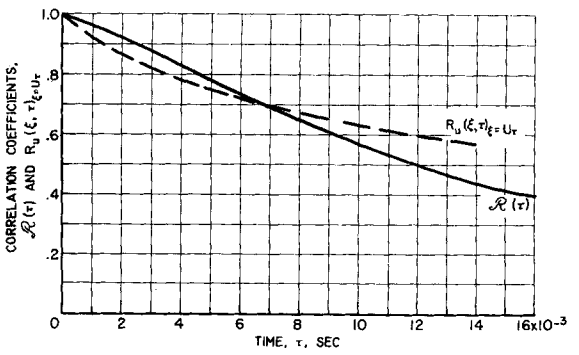

Fig. 10. Comparison of measured Lagrangian and general Eulerian correlation coefficients, $U \approx 73$ ft./sec.

instantaneous two-wire Eulerian correlation ($\tau = 0$). Finally, and most important of all, the true Lagrangian correlation coefficient inferred from diffusion measurements at approximately this flow condition (Figure 7, $U_c = 72.6$) does resemble the general Eulerian correlation taken along $\xi = U\tau$, shown by Figure 10. The evidence is of course preliminary, but it would appear that future research along these lines might lead to simple empirical relations between the Lagrangian correlation and the new Eulerian correlation, which are compared here for the first time.

SUMMARY AND CONCLUSIONS

The following remarks summarize the findings of this experimental study of turbulent diffusion in the core of fully developed pipe flow:

1. G. I. Taylor's theory of diffusion by continuous movements correctly predicted two basic characteristics of the turbulent diffusion in the pipe core. The apparent eddy diffusivity increased from zero at the heat source to a constant asymptotic value far downstream. The usual assumption used with Taylor's theory was also verified; the diffusion profiles were Gaussian within experimental precision for all distances downstream of the heat source.

2. The Lagrangian single-particle correlation coefficients which are defined in Taylor's theory were inferred from the diffusion data. The Lagrangian correlations have shapes similar to the Eulerian space correlation coefficients measured by hot-wire anemometers. An exception to the latter statement occurs for small values of the correlations, where the Lagrangian coefficient apparently approaches zero monotonically and the Eulerian correlation $f(\xi)$ dips below zero to slightly negative values before approaching a zero-value asymptote.

3. An empirical factor K was found which transforms the distance axis ξ of the Eulerian correlation coefficient into the time coordinate τ of the Lagrangian correlation coefficient by

$$\xi = \frac{\sqrt{\overline{v^2}_{La}}\,\tau}{K}$$

The factor K is approximately constant over the entire range of ξ and τ at each flow condition. However the factor varied from about 0.28 to 0.14 as the root-mean-square turbulent velocity $\sqrt{\overline{u^2}}$ varied from 2.1 to 4.8 ft./sec. The corresponding range of mean flow velocities U_c was 72.6 to 160 ft./sec.

4. A reanalysis of Mickelsen's data (12) on helium diffusion in pipe-core turbulence gave empirical factors K which were similar with the results of the present work.

5. Preliminary measurements of a new general Eulerian correlation coefficient $R_u(\xi, \tau)$ are reported. $R_u(\xi, \tau)$ relates two fluid particles at two times in space. When one uses an approximation for the Lagrangian derivative suggested by J. M. Burgers (39), $R_u(\xi, \tau)$ is shown to approach the true Lagrangian correlation coefficient. The preliminary measurements verified this prediction for the one-flow condition investigated ($U_c \approx 73$ ft./sec.).

6. The turbulence intensities reported by previous workers using hot-wire anemometers are probably low by about 30% in pipe flow at high Reynolds numbers. The reason for this discrepancy is that the traditional anemometer calibrations were based on King's equation. This relation overestimates the actual anemometer sensitivity and gives intensities which are too low. Fortunately all nondimensional ratios of the turbulent velocity, such as correlation coefficients and spectra, are not affected by this calibration error.

ACKNOWLEDGMENT

L. V. Baldwin's senior colleagues in turbulence research at the National Aeronautics and Space Administration, Lewis Research Center, aided with both counsel and criticism. Mr. James C. Laurence, Mr. William R. Mickelsen and Mr. V. A. Sandborn were especially helpful. Mr. Bert Henry directed the computing. This report was prepared with the financial support of the National Aeronautics and Space Administration graduate study program.

NOTATION

a = pipe radius, ft.
c = concentration
$\bar{c}$ = mean molecular velocity, ft./sec.
c_p = isobaric specific heat, B.t.u./(lb.)(°F.)
D = eddy diffusivity, sq. ft./sec.
D_{mol} = molecular diffusivity, sq.ft./sec.
$f(r)$ = normal Eulerian correlation coefficient defined by Karman-Howarth (5), dimensionless
$g(r)$ = transverse Eulerian correlation coefficient defined by Karman-Howarth (5), dimensionless
K = empirical factor in Equation (10), dimensionless
k = thermal conductivity for air, B.t.u./(sec.)(ft.)(°F.)
L_f = Eulerian integral scale, ft.
$\mathcal{L}$ = Lagrangian integral scale, ft.
l = mean free path for air, ft.
N_{Re} = $\rho U 2a/\mu$, Reynolds number, dimensionless
R = correlation coefficient, dimensionless
$R_r(\xi, \tau)$ = general Eulerian correlation coefficient in space and time for lateral turbulent velocity, dimensionless
$\mathcal{R}$ = Lagrangian single - particle correlation coefficient, dimensionless
T = temperature, °R.
t = time, sec.
U = mean air velocity, ft./sec.
$\overline{u}$ = time mean longitudinal turbulent velocity, $\overline{u} \equiv 0$
$\overline{u^2}$ = longitudinal turbulent velocity variance, sq.ft./sec.^{2}
$\overline{v^2}$ = lateral turbulent velocity variance, sq.ft./sec.^{2}
X = particular point in x-direction
x = axial coordinate
Y = particular point in y-direction

Y^2 = horizontal displacement variance, sq.ft.
y = horizontal coordinate
Z = particular point in z-direction
z = vertical coordinate

Greek Letters

α = thermal diffusivity, sq.ft./sec.
Δ = difference
μ = air viscosity lb.(m)/(ft.)(sec.)
ξ = separation distance in x coordinate
ρ = air density lb.(m)/(cu. ft.)
τ = time, sec.

Superscripts

bar = average

Subscripts

a, b, c, d = particular fluid particles
c = axial center line
f = Eulerian correlation, $f(\xi)$
La = Lagrangian, averaged time histories of many single-fluid-particle motions
n = zero correlation
tot = total dispersion
u, v, w = particular turbulent velocities
0 (zero) = peak or center line

LITERATURE CITED

1. Taylor, G. I., *Proc. Roy. Soc. (London)*, **151**, 421 (1935).
2. Batchelor, G. K., "The Theory of Homogeneous Turbulence," Cambridge Univ. Press, England (1956).
3. Townsend, A. A., "The Structure of Turbulent Shear Flow," Cambridge Univ. Press, England (1956).
4. Agostini, L., and J. Bass, *Natl. Advisory Comm. Aeronaut., Tech. Memo. 1377* (1955); Translated from *Pub. Sci. et Tech. du Ministère de L'Air*, No. 237 (1950).
5. von Karman, T., and L. Howarth, *Proc. Roy. Soc. (London)*, **A164**, 192 (1938).
6. Robertson, H. P., *Proc. Camb. Phil. Soc.*, **36**, 209 (1940).
7. Taylor, G. I., *Proc. London Math. Soc.*, **20**, 196 (1922).
8. Frenkiel, F. N., in "Advances in Applied Mechanics," Vol. III, p. 61, Academic Press, New York (1953).
9. Scull, Wilfred E., and W. R. Mickelsen, *Natl. Advisory Comm. Aeronaut., Rep. 1300* (1957).
10. Kalinske, A. A., and C. C. Pien, *Ind. Eng. Chem.*, **36**, 220 (1944).
11. Towle, W. L., and T. K. Sherwood, *ibid.*, **31**, 457 (1939).
12. Mickelsen, W. R., *Natl. Advisory Comm. Aeronaut., Tech Note 3570* (1955).
13. Hanratty, T. J., *et al., A.I.Ch.E. Journal*, to be published.
14. Schubauer, G. B., *Natl. Advisory Comm. Aeronaut., Rep. 524* (1935).
15. Uberoi, M. S., and S. Corrsin, *ibid., Rep. 1142* (1953).
16. Townsend, A. A., *Proc. Roy. Soc. (London)*, **224**, 417 (1954).
17. Frenkiel, F. N., and I. Katz, *J. Meteorol.*, **13**, 388 (1956).
18. Hay, J. S., and F. Pasquill, *J. Fluid Mech.*, **2**, 299 (1957).
19. Vi-Cheng, Liu, *J. Meteorol.*, **13**, 399 (1956).
20. Brier, G. W., *Meteorol. Monographs*, **1**, 15 (1951).
21. Baldwin, L. V., Ph.D. thesis, Case Inst. Tech., Cleveland, Ohio (1959).
22. Laurence, J. C., and L. G. Landes, *Natl. Advisory Comm. Aeronaut., Tech. Note 2843* (1952).
23. Sandborn, V. A., *ibid., Tech. Note 3266* (1955).
24. Carlson, E. R., C. C. Conger, J. C. Laurence, E. H. Meyn, and R. A. Yocke, *Proc. Inst. Radio Engrs.*, 47 (1959).
25. Baldwin, L. V., *Natl. Advisory Comm. Aeronaut., Tech. Note 4369* (1958).
26. ———, V. A. Sandborn, and J. C. Laurence, *Am. Soc. Mech. Engrs.*, Paper No. 59-HT-5.
27. Cybulski, R. J., and L. V. Baldwin, *Natl. Aeronaut. Space Admin., Memo 4-27-59E* (1959).
28. Baldwin, L. V., V. A. Sandborn, and J. C. Laurence, *Trans. Am. Soc. Mech. Engrs., Series C*, **82**, No. 2, p. 77 (1960).
29. Corrsin, S., *Natl. Advisory Comm. Aeronaut., Tech. Note 1864* (1949).
30. Grant, H. L., and J. C. T. Nisbet, *J. Fluid Mech.*, 263 (1957).
31. Lin, C. C., *Navord Rep. 2306* (March, 1952).
32. Laurence, James C., *Natl. Advisory Comm. Aeronaut., Rep. 1292* (1956).
33. Hilsenrath, J., *et al., Natl. Bur. Standards (U.S.), Circ. 564* (Nov. 1, 1955).
34. Batchelor, G. K., and A. A. Townsend, "Turbulent Diffusion. Surveys in Mechanics," Cambridge Univ. Press, England (1956).
35. Mickelsen, W. R., *J. Fluid Mech.*, **7**, 397 (1960).
36. Einstein, Albert, "Investigations on the Theory of the Brownian Movement," p. 13, Methuen Press, London (1927); Dover Press, London (1956).
37. Dryden, Hugh L., *Ind. Eng. Chem.*, **31**, 415, (1939).
38. Taylor, G. I., *Proc. Roy. Soc. (London)*, **A223**, 446 (1954).
39. Burgers, J. M., *Rep. No. E-34.1*, Calif. Inst. Technol., Pasadena (July, 1951).
40. Bass, J. "Space and Time Correlations in a Turbulent Fluid, I and II," Vol. II, p. 55, Univ. of Calif. Public. in Statistics (1954).

Manuscript received January 14, 1960; revision received April 22, 1960; paper accepted April 27, 1960. Paper presented at A.I.Ch.E. San Francisco meeting.

APPENDIX

Approximate Relation Between Eulerian Space-Time Correlation and Lagrangian Single-Particle Correlation

Consider the Taylor series expansion of the new Eulerian function about the origin [that is $R_v(\xi) = R_v(\tau) = R_v(\xi, \tau) = 1.0$] in any arbitrary direction given by r and θ an a map of isocorrelation curves in time and space. The following relations hold:

$$\left.\begin{aligned} \xi &= r\cos\theta \\ \tau &= r\sin\theta \\ \tan\theta &= \frac{\tau}{\xi} \equiv \frac{1}{V} \end{aligned}\right\} \qquad \text{(A-1)}$$

were V has the units of velocity. The expansion of this function about the origin (retaining only second-order terms for this example) is

$$R(r,\theta) = R(0,\theta) + \frac{r}{\overline{v^2}}\left[\cos\theta\left.\frac{\partial R(r,\theta)}{\partial\xi}\right|_0 + \sin\theta\left.\frac{\partial R(r,\theta)}{\partial t}\right|_0\right] + \frac{1}{2}\frac{r^2}{\overline{v^2}}\left[\cos^2\theta\left.\frac{\partial^2 R(r,\theta)}{\partial\xi^2}\right|_0 + 2\sin\theta\cos\theta\left.\frac{\partial^2 R(r,\theta)}{\partial\xi\partial t}\right|_0 + \sin^2\theta\left.\frac{\partial^2 R(r,\theta)}{\partial t^2}\right|_0\right] + \ldots \qquad \text{(A-2)}$$

Taylor (*1*) demonstrated that the Eulerian correlation $R(\xi)$ is an even function due to the homogeneity of the turbulent field. The proof is straightforward:

$$\frac{\partial R}{\partial\xi} = \overline{v(x)\left(\frac{\partial v}{\partial x}\right)_{x+\xi}} \qquad \text{(A-3)}$$

or at the origin

$$\left.\frac{\partial R}{\partial\xi}\right|_0 = \overline{v\frac{\partial v}{\partial x}} = \frac{\partial}{\partial x}\overline{\left(\frac{v^2}{2}\right)} = 0 \qquad \text{(A-4)}$$

This result follows from the fact that $\overline{v^2} \neq f(x)$. A similar argument for stationary turbulence shows that $\partial R(r,\theta)/\partial t = 0$. Therefore the expansion will be for an even function:

$$R(r,\theta) = 1.0 + \frac{1}{2}\frac{r^2}{\overline{v^2}}\left[\cos^2\theta\left.\frac{\partial^2 R(r,\theta)}{\partial\xi^2}\right|_0 + 2\sin\theta\cos\theta\left.\frac{\partial^2 R(r,\theta)}{\partial t\partial\xi}\right|_0 + \sin^2\theta\left.\frac{\partial^2 R(r,\theta)}{\partial t^2}\right|_0\right] + \ldots \qquad \text{(A-5)}$$

For the second derivatives at the origin

$$\left.\frac{\partial^2 R(r,\theta)}{\partial\xi^2}\right|_0 = \overline{v\frac{\partial^2 v}{\partial x^2}} = \frac{\partial}{\partial x}\overline{\left(v\frac{\partial v}{\partial x}\right)} - \overline{\left(\frac{\partial v}{\partial x}\right)^2} \qquad \text{(A-6)}$$

But for homogeneous turbulence the mean value of a velocity derivative with respect to x is zero (A-4), so Equation (A-6) is simply

$$\left.\frac{\partial^2 R(r,\theta)}{\partial\xi^2}\right|_0 = -\overline{\left(\frac{\partial v}{\partial x}\right)^2} \qquad \text{(A-7)}$$

An analogous argument for stationarity may be made to show that

$$\left.\frac{\partial^2 R(r,\theta)}{\partial t^2}\right|_0 = -\overline{\left(\frac{\partial v}{\partial t}\right)^2} \qquad \text{(A-8)}$$

The other derivative may be developed as follows:

$$\frac{\partial}{\partial t}\left[\frac{\partial R(r,\theta)}{\partial \xi}\right]_0 = \overline{v\frac{\partial^2 v}{\partial x \partial t}}$$

$$= \overline{\frac{\partial v}{\partial t}\frac{\partial v}{\partial x}} + \overline{\frac{\partial}{\partial t}\left(v\frac{\partial v}{\partial x}\right)} \qquad \text{(A-9)}$$

For stationary turbulence the Eulerian space derivative is not a function of time, so

$$\frac{\partial^2 R(r,\theta)}{\partial \xi \partial t}\bigg|_0 = -\overline{\frac{\partial v}{\partial t}\frac{\partial v}{\partial x}} \qquad \text{(A-10)}$$

Combining Equations (A-5), (A-7), (A-8), and (A-10) and noting that Equation (A-1) may be used to eliminate the trigonometric functions one obtains

$$R_v(r,\theta) = 1 - \frac{\tau^2}{2v^2}\left[\overline{V^2\left(\frac{\partial v}{\partial x}\right)^2} + 2V\overline{\frac{\partial v}{\partial x}\frac{\partial v}{\partial t}} + \overline{\left(\frac{\partial v}{\partial t}\right)^2}\right] + \ldots \qquad \text{(A-11)}$$

For the special case of θ, where $V = U$, Equation (A-11) becomes

$$R_v(\xi,\tau)\big|_{\xi=U\tau} = 1 - \frac{\tau^2}{2v^2}\left[U^2\overline{\left(\frac{\partial v}{\partial x}\right)^2} + 2U\overline{\frac{\partial v}{\partial x}\frac{\partial v}{\partial t}} + \overline{\left(\frac{\partial v}{\partial t}\right)^2}\right] + \ldots \qquad \text{(A-12)}$$

When one recalls Burger's approximation of the Lagrangian derivative

$$\frac{dv}{dt} \cong \frac{\partial v}{\partial t} + U\frac{\partial v}{\partial x} \qquad \text{(A-13)}$$

or

$$\overline{\left(\frac{dv}{dt}\right)^2} \cong U^2\overline{\left(\frac{\partial v}{\partial x}\right)^2} + 2U\overline{\frac{\partial v}{\partial x}\frac{\partial v}{\partial t}} + \overline{\left(\frac{\partial v}{\partial t}\right)^2} \qquad \text{(A-13}a\text{)}$$

Substituting Equation (A-13a) into (A-12) and assuming the approximate equivalence of single-particle time averages to two-particle space averages one gets

$$R_v(\xi,\tau)\big|_{\xi=U\tau} \cong 1 - \frac{\tau^2}{2v^2}\overline{\left(\frac{dv}{dt}\right)^2} + \ldots \qquad \text{(A-14)}$$

Or letting $\overline{v^2} \cong \overline{v^2_{La}}$ one gets the desired relation:

$$R_v(\xi,\tau)\big|_{\xi=U\tau} \cong \mathcal{R}(\tau) \qquad \text{(A-15)}$$

Equation (A-15) verifies the remark that to the same approximation as Equation (A-13) the general Eulerian correlation along $\xi = U\tau$ will approach the true Lagrangian correlation coefficient in a homogeneous, isotropic, and stationary turbulence.

Physically $R_v(\xi,\tau)\big|_{\xi=U\tau}$ corresponds to the Eulerian autocorrelation as measured by a fixed probe in a hypothetical box of turbulence which is homogeneous, isotropic, and stationary. Bass (*40*) has given a theoretical development for Eulerian space-time correlations which is comparable to that of Kármán and Howarth (*5*) for the more familiar case of Eulerian space correlations.

A Modification of the Momentum Transport Hypothesis

WILLIAM N. GILL and MARVIN SCHER

Syracuse University, Syracuse, New York

A continuous velocity distribution is derived which is based on an arbitrary modification of Prandtl's mixing length expression. The resulting velocity distribution agrees well with experiments for transition and fully developed turbulent flow throughout the entire cross section of the conduit. Furthermore the mixing length expression applies to parallel flow in smooth circular tubes and between infinite parallel plates with the same set of constants.

Prandtl's famous momentum transport hypothesis has been successful in predicting velocity distributions in the turbulent core of bounded or conduit flow. Usually velocity distribution expressions derived on the basis of this hypothesis neglect the shear stress variation across the conduit, the molecular viscosity term, and more important the viscous dampening effect of the wall on eddy properties near the wall. Van Driest (*15*) considered viscous dampening to be an exponential function of the distance from the wall and showed how this dampening is influenced by surface roughness. However the extent of viscous dampening has been clearly demonstrated by the experimental work of Sage and coworkers (*1, 8, 9*) to be a function of the Reynolds number and has not been successfully explained except on an empirical basis by Rothfus and Monrad (*11*). Consequently a derivation of the generalized velocity distribution expression is needed which accounts for the previously mentioned effects within the framework of Prandtl's hypothesis. The following treatment has several advantages over existing velocity distribution expressions which are:

1. A single continuous function represents the velocity distribution from the wall to the center of the channel for both flat plates and circular tubes.
2. A zero velocity gradient at the center of the channel is obtained.
3. The Reynolds number effect on the velocity distribution is accounted for and will be seen to be most pronounced in the transition flow region.
4. The velocity distribution reduces to the Hagen-Poiseuille equation at $N_{Re} = 1{,}800$ for circular tubes and at $N_{Re} = 4{,}800$ for flat plates.

It has been shown that eddy properties very near a solid boundary may be more precisely determined from heat and mass transfer measurements at high Schmidt or Prandtl numbers than by velocity distribution studies (*3, 5, 10*). However this discussion is intended only to describe these approximately in the immediate vicinity of the wall and at the same time resolve the apparent discrepancies between turbulent transition flow in tubes and between parallel plates which have been observed as a result of careful measurements. Velocity distribution explorations by Deissler (*2*) and Laufer (*4*) for turbulent flow in tubes and between flat plates indicate a single valued relation between u^+ and y^+ over